Variability of Shallow Water Masses of the Northern and Tropical Oceans as Viewed in Nine Ocean Analyses

James A. Carton[1], Gennady A. Chepurin[1], and You-Soon Chang[2]

August 29, 2008

[1]Department of Atmospheric and Oceanic Science
University of Maryland
College Park, MD 20742
carton@atmos.umd.edu

[2]Geophysical Fluid Dynamics Laboratory
Box 308
Princeton, NJ 20854

Abstract

This paper explores the mean state and variability of upper ocean water properties in the northern and tropical oceans during the years 1962-2001 as represented in nine ocean analyses. We begin by examining the winter-spring characteristics of SST and the mixed layer which regulate the sources water masses to the upper ocean. We then compare variability of the depth of constant density surfaces, particularly the 25.5σ surface to that described in previous studies focusing on representative climate phenomena. In the western North Pacific all analyses show a decadal succession of depth anomalies which circulate clockwise around the subtropical gyre consistent with the behavior previously described by *Miller and Schneider (2000)*. On longer timescales the 25.5σ surface undergoes a reduction in its zonal slope between the intervals 1970-1977 and 1990-1999, a reduction that *McPhaden and Zhang (2002)* associate with a slowing down of the shallow meridional overturning circulation in this basin. Comparisons with time series records at Hawaii and Bermuda show that while the analyses are able to reproduce observed responses to anomalous surface forcing, they differ significantly in the far field representation of those anomalies. In the subpolar North Atlantic five of the analyses are able to reproduce observed the Great Salinity Anomaly fresh events of the 1970s and 1980s. Examination of these five show three that allow a significant role for freshwater transport from the Arctic Ocean, while two suggest a dominant role for local sources of freshwater.

1. Introduction

In their 1997 study *Yasuda and Hanawa* found decadal changes in the temperature and salinity of the upper ocean water masses of the North Pacific that occur in concert with decadal changes in North Pacific climate. These changes in stratification alter the temperature of water entrained into the winter mixed layer, thus providing a mechanism for decadal climate variability. Indications of decadal changes in other upper ocean water masses have also been seen in the tropical Pacific and North Atlantic (e.g. *Lazier, 1995; Joyce and Robbins, 1996; McPhaden and Zhang, 2002*). Here we apply a set of nine ocean analyses spanning part or all of the period 1962-2001 to examination of changes in the stratification of the upper layers of these northern and tropical oceans. Our goals are to explore representation of key subseasonal changes in water masses in different analyses, and suggest possible causes of differences in representation as a way of understanding the uncertainty in the analysis estimates.

The upper ocean water masses of the northern and tropical oceans have received much of the attention in the scientific literature and are vastly better-sampled than their Southern Hemisphere counterparts. For these reasons we restrict our attention to the northern and tropical oceans. The North Pacific and Atlantic have mixed layers that are shallow in summer, deepening throughout fall and winter to a maximum depth in excess of 200m in late winter and early spring as the result of reductions in surface buoyancy flux and increases in turbulent mixing (*de Boyer Montégut et al.*, 2004). High levels of freshwater flux in the North Pacific lead to the formation of wintertime >10m thick salinity barrier layers north of 40^{o}N, while in the eastern North Atlantic the deeper winter mixed layers

show significant compensation between salinity and temperature stratification due to the northward advection of warm salty water over cooler fresher water *(de Boyer Montegut et al.*, 2007).

In the North Pacific the highest year-to-year variability of the maximum seasonal mixed layer depth occurs in the region between the dateline and 150^{o}W and 35^{o}-45^{o}N, and is strongly correlated in time with the Index of the Pacific Decadal Oscillation (*Carton et al., 2008*). In the North Atlantic the maximum spatially coherent year-to-year variability of seasonal mixed layer depth occurs in a zone extending along the eastern edge of the Gulf Stream in the western subtopics northeastward toward the eastern subtropics. But, in contrast to the North Pacific, the mixed layer depth variability in this region is not closely related to local variations in wind speed and does not result in spatially coherent variations in winter SST.

We next review the characteristics of constant density surfaces. In the North Pacific the time mean depth of the 24.5σ surface, which lies close to the top of North Pacific Subtropical Mode Water (σ = 24.5-25.9) and North Pacific Eastern Subtropical Mode Water (σ = 24-25.4; *Bingham and Suga, 2006*) reaches a maximum depth of 200m in the northwestern tropical Pacific, shallowing to less than 50m north of 30^{o}N as well as in eastern North Pacific, and also shallowing in a narrow band of latitudes along a ridge in the thermocline at 10^{o}N latitude. In these regions where the 24.5σ surface is shallow the water on this surface is cool and fresh (< 34.4psu). Approaching the equator the 24.5σ surface deepens again with elevated values of temperature and salinity.

In the North Pacific the 25.5σ surface lies close to the lower boundary of North Pacific Subtropical Mode Water and North Pacific Eastern Subtropical Mode Water. The density surface reaches its maximum depth somewhat further north and west of the maximum depth of the 24.5σ surface, and at its maximum depth it exceeds 300m. The 25.5σ surface is also shallow (<100m) in a latitude band around 10^{o}N and near the west coast of the United States, deepening somewhat at equatorial latitudes. One study referred to later, by *Miller and Schneider (2000)*, shows that displacements of the depth of the 25.5σ surface by density anomalies generated in the central North Pacific travel clockwise around the subtropical gyre along constant potential density surfaces. These displacements are shown by *Miller and Schneider* to impact SST and thus the climate of the Kuroshio/Oyashio Extension region. The 26.5σ density surface falls within the lower depths of a third water mass known as North Pacific Central Mode Water. This latter water mass is formed between the subpolar front and the Kuroshio (35-45^{o}N), and is confined west of 150^{o}W (*Bingham and Suga, 2006)*. *Yasuda and Hanawa (1997)* examine changes in the distribution of the deeper North Pacific Central Mode Water in the decades before and after 1976 and conclude that this mode water cooled and spread with time. They also explore potential causes of these changes and identify increased winter heat loss as well as increased heat advection in the Kuroshio and central Pacific regions due to a speed-up of the subtropical gyre.

McPhaden and Zhang (2002) also examine longer decadal timescale changes in the depth of isopycnal surfaces associated with changes in the shallow meridional overturning

circulation. They suggest that a reduction in the climatological westward tilt of the 25.0σ surface between the 1970s and 1990s, which they detect in their own analysis of historical hydrography, is the result of a reduction in equatorward heat transport and equatorial upwelling during these decades. The possibility of decadal changes in tropical water masses and their potential association with decadal changes in ENSO, indeed, continues to be the subject of active research (*Kleeman et al., 1999; Nonaka et al., 2002; Schneider, 2004*).

The waters of the North Atlantic are saltier and denser than those of the North Pacific and in this basin the 26.5σ surface defines the core of the main subtropical water mass, the (18^{o}C) North Atlantic Subtropical Mode Water (*Hanawa and Talley, 2001; Climode, 2008*). The long hydrographic time series near Bermuda provides a unique record of North Atlantic Subtropical Mode Water variability. Potential vorticity (inversely related to layer thickness) at this location was high between 1972-1976 and again in the mid-1980s as a result of a succession of warm winters during which the rate of formation of the water mass was reduced (*Joyce and Robbins, 1996; Joyce et al., 2000*). To the east a second subtropical North Atlantic water mass known as Madeira Mode Water is formed in the region of the Madeira Islands (33^{o}N, 16^{o}W) (*Ratsimandresey, et al., 2001*) with slightly heavier densities (26.5-26.8σ, Siedler *et al., 1987*). The properties of this mode water also change over time. The severe winter of 1988-9, for example, produced colder temperatures.

Further north a series of subpolar mode waters have been examined in recent papers by *Brambilla and Talley (2008)* and *Brambilla et al. (2008)*. However the most striking year-to-year variability in the upper ocean has been observed in the Labrador Sea where the salinity of the surface layer (0-250m) is dominated by salinity 'Great Salinity Anomaly' decreases of 0.2psu during 1967-1971 and again 1978-1985. Several causes have been suggested, including anomalous freshwater export from the Arctic in the forms of sea ice and reduced salinity water (*Proshutinsky and Johnson 1997; Belkin, 2004*) and local freshwater fluxes (*Houghton and Visbeck, 2002)*. The low salinity anomalies advect counterclockwise around the subpolar gyre, so that the Great Salinity Anomaly that appeared in the Labrador in 1967-1971 reappears in the Norwegian Basin in the mid-1980s (*Nilsen and Falck, 2003*).

In the past several years, a number of analyses of ocean properties spanning multiple decades at monthly resolution have become available which offer exciting potential to allow diagnostic studies of climate phenomena. Here we examine an ensemble of nine such analyses, including six using sequential data assimilation together with a numerical ocean circulation model, one using sequential assimilation applied to a coupled atmosphere/ocean model, and one using a 'no-model' objective analysis in which climatology provides a first guess. Finally, we include a synthesis analysis using 4DVar with both a (forward) numerical model and its tangent linear adjoint. This ensemble of nine analyses is used to examine a selection of climate phenomena in the North and tropical Pacific and North Atlantic with the goal of exploring the limits of the historical

observational record and the dependence of the representation of climate variability on the choice of analysis technique.

2. Methods and Data

As just mentioned, the nine analyses of historical ocean circulation, summarized in **Table 1**, can be divided by estimation technology into four types. The 'no-model analysis', UK-OI[1], is constructed by objectively analyzing the historical profile observation set assuming a climatological first guess and has 1^ox1^o horizontal resolution. We examine five analyses constructed using sequential estimation techniques with an ocean general circulation model to provide a first guess, CERFACS[2], GODAS[3], ECMWF[4], INGV[5], SODA[6], and UK-FOAM[7]. CERFACS, INGV, and ECMWF have 2^ox2^o horizontal resolution in midlatitude and higher tropical resolution. Of these CERFACS and INGV have somewhat higher vertical resolution. GECCO[8], GFDL, GODAS, and UK-FOAM have 1^ox1^o horizontal resolution in midlatitudes, and of these all but GECCO have refined meridional resolution in the tropics. Of this group of four, GODAS has the highest vertical resolution. The analysis with the finest horizontal resolution is SODA, with 0.4^ox0.25^o resolution in the tropics and further refinement at high latitudes in order to maintain a roughly isotropic grid-point distribution. Most models include a full Arctic Ocean. The exceptions are GODAS and GECCO which limit their domain to the region south of 65^oN and 79.5^oN respectively.

[1] United Kingdom Optimal Interpolation, *Bell (2000)* and *Bell et al. (2004).*
[2] Instituto Nazionale di Geofisica e Volcanologia, Bellucci *et al. (2007).*
[3] National Centers for Environmental Prediction Global Ocean Data Assimilation, *Behringer (2005).*
[4] European Centre for Medium Range Weather Forecasts, Balmaseda et al. (2007).
[5] The European Centre for Research and Advanced Training in Scientific Computation, *Davey (2005).*
[6] Simple Ocean Data Assimilation, *Carton and Giese (2008).*
[7] United Kingdom Forecasting Ocean Assimilation Model, *Bell (2000)* and *Bell et al. (2004).*
[8] Global Estimation of Circulation and Climate Experiment, *Kohl and Stammer (2008).*

The analyses differ in the surface forcing used. Five of the analyses; CERFACS, ECMWF, INGV, SODA and UK-FOAM; use winds provided by the European Centre for Medium Range Weather Forecasts ERA-40 reanalysis (*Uppala, et al., 2005*). Four of these also use freshwater fluxes from ERA-40 (modified in the tropics, see **Table 1**), while SODA combines Global Precipitation Climatology Project rainfall (*Adler, 2003*) with a bulk parameterization of evaporation. GECCO begins with National Centers for Environmental Prediction (NCEP) reanalysis (*Kalnay et al., 1996*) fluxes and modifies those as a result of the 4DVar procedure. GODAS uses NCEP reanalysis 2 (*Kanamitsu et al., 2002)* fluxes. GFDL[9] gets their fluxes as a by-product of the ocean-atmosphere coupled model. *Carton and Santorelli (2008)* note some differences among the ocean analyses such as changes in temperature associated with the introduction of satellite atmospheric soundings in the 1970s into the wind analysis procedure, which cause step-like changes in the surface winds and thermodynamic fluxes during this decade.

The analyses also differ in the ocean observation sets used. Five analyses, CERFACS, ECMWF, INGV, and UK-FOAM, and UK-OI are part of the ENACT program (*Davey, 2005*) and use a common profile data set that includes sophisticated bias corrections (*Thadathil et al., 2002*). Most of the others rely on one or another of the versions of the World Ocean Database (the latest, WOD05, is described in *Boyer et al., 2006*). Differences among the profile data sets and associated corrections are summarized in *Carton and Santorelli (2008)* along with a discussion of the important issue of time-dependent bias in a major component of the profile observation set.

[9] Geophysical Fluid Dynamics Laboratory (*Zhang et al., 2007; 2008a,b*)

But, likely the most important differences in the observation sets is the introduction of satellite altimeter sea level, available continuously since 1991, in GECCO and GODAS. Introduction of this data may account for the warming in the North Pacific observed in GECCO in the 1990s. Many of the analyses also include satellite SST. For CERFACS, GECCO, GFDL, GODAS, and INGV these data enter indirectly through the use of a gridded SST product. SODA assimilates the night-time SST observations into their mixed layer temperature estimates.

Each analysis output is reduced to monthly averaged temperature and salinity for whatever portion of our period of interest, 1962-2001, is available (see **Table 1**). CERFACS, ECNWF, INGV, UK-FOAM, and UK-OI outputs have been interpolated to a common $1^{o}x1^{o}$ degree grid at standard vertical levels (the interpolation has been carried out by the analysis authors). The anomalies examined in the Results Section are generally computed relative to the 16-year period 1980-1995.

In our comparisons below we include discussion of the differences between the analyses and the observations. To construct difference maps the analysis fields are linearly interpolated to the horizontal location and time of the high accuracy WOD05 conductivity-temperature-depth and station profiles. The analysis-minus-observation differences are then accumulated over our period of interest and gridded onto a uniform horizontal grid to facilitate analysis. When evaluating the uppermost analysis temperature we compare against two separate data sets. The first is the uppermost

temperature value of the profile set mentioned above. The second is the HADSST2 bulk SST data set (*Rayner et al., 2003*). We include both comparisons because in some locations analyses may be adjusted to match one or another of these data sets (Semyon Grodsky, personal communication, 2008).

3. Results

We begin by considering the time-mean properties focusing on winter-spring (JFM) mixed layer (**Fig.1a**) and SST (**Fig.1b**) because of the relationship of these variables to the sub-mixed layer ocean and to decadal climate. Many of the analyses have winter-spring mixed layers that are shallower than observed in the northern North Pacific and deeper than observed in the northern and western subtropical Atlantic. In the northern North Pacific a temperature inversion is observed to prevail in winter as a result of near surface freshening and intense cooling. In this region analyses with insufficiently deep mixed layers also have a low salinity inversion layer which is too shallow. Those analyses with shallow low salinity layers in this region, such as CERFACS and INGV also tend to have SSTs that are significantly cooler than observed (**Fig. 1b**). The exceptionally shallow mixed layers produced by UK-OI are the result of a temperature inversion of a few tenths of a degree in the upper 30m. This nearsurface temperature inversion is sufficiently large to give unrealistically shallow mixed layer depth estimates (as the result of our use of a $|0.2^{o}C|$ criterion for defining the mixed layer base).

Along the equator in the eastern equatorial Pacific several analyses, including CERFACS, GODAS, SODA, and UK-FOAM, have surface temperatures which are

cooler by >0.25^{o}C than observed bulk SST. However, this systematic difference is less apparent when these analyses are compared to observed profile temperatures at the uppermost levels. Several analyses have a 0.25^{o}C warm winter-spring SST bias in the subtropical Pacific including CERFACS, GFDL, and SODA. GECCO is anomalously warm along the subtropical front, but 0.25-0.5^{o}C cool elsewhere.

In the subtropical North Atlantic GFDL and GECCO are notable for having an unusually deep winter mixed layer in mid-basin (**Fig. 1a**). In both analyses this deep mixed layer occurs in a region where a cool error of 1^{o}C (**Fig. 1b**) reduces SST to close to the 18^{o}C temperature of North Atlantic Subtropical Mode Water (normally present below the mixed layer), allowing this mode water to be exposed to the surface in winter. Analyses such as CERFACS with shallower mixed layers in the winter North Atlantic have somewhat higher SSTs. All analyses show SSTs that are warmer than observed on the northwest (inshore) side of the Gulf Stream.

We next consider the time mean depth and salinity of the 25.5σ surface in the analyses relative to the contemporaneous profile observations (**Fig. 2**). Interestingly, although GECCO has generally cool SSTs in the North Pacific during winter the 25.5σ surface is 10-30m too deep reflecting a dramatic warming of its thermocline in the 1990s. An anomalous deepening is also evident in the north tropical Atlantic in GECCO, GODAS, INGV, and SODA. Among the other analyses a <10m positive depth error is evident in the eastern North Pacific and a <10 negative depth error is evident in the western North

Pacific indicating that the zonal slope of the 25.5σ surface is weaker in the analyses than indicated by the profile observations.

We next consider the spatial distribution of sub-seasonal variability of constant density surfaces about their annual mean (**Fig.3** shows the 3-year low pass filtered depth variability of both the 25.5σ and 26.5σ surfaces). All analyses show strong variability of the 26.5σ surface, in excess of 45m, in the subtropical North Atlantic south of the Gulf Stream where North Atlantic Subtropical and Madeira Mode Waters are found. The strongest variability in the eastern basin occurs in GFDL. Much of the variability of GFDL in this region is associated with a multi-decadal freshening trend.

In the North Pacific all analyses show variability of the depth of the 25.5σ and 26.5σ surfaces in the western subtropical gyre with the maximum for 25.5σ displaced to the south of the maximum for 26.5σ (**Fig. 3**). To the north in the Pacific **Fig. 3** reveals depth variability in excess of 15m in CERFACS, ECMWF, and SODA. *Miller and Schneider (2000)* examine thermocline variability as represented in the analysis of *White (1995)* and suggest that much of this variability is in the form of shallow and deep anomalies that form at northern latitudes and travel counterclockwise around the subtropical gyre along lines of constant potential vorticity. Here we find qualitatively similar depth anomalies in all analyses we examine (**Fig. 4**). GFDL has significant equatorial anomalies which, as in the eastern North Atlantic, partly result from a multi-decadal freshening trend evident in several geographic locations.

In addition to decadal variability the depth of the 25.5σ surface shows long-term changes (**Fig. 5**) which *McPhaden and Zhang (2002)* identify based on their own analysis of the historical hydrographic record and associate with changes in the shallow meridional overturning circulation of the tropical Pacific. Between the 1970s and 1990s our ensemble of analyses also show a deepening of the eastern subtropics by up to 30m and a corresponding shallowing of the western tropics by more than 10m. *McPhaden and Zhang* link these changes to climate variability through their impact on tropical stratification. Along the equator comparison of water properties of the ensemble between these decades shows a reduction in density nearsurface at all longitudes and an increase in density at thermocline depths west of 180^{o}W (**Fig. 6**). This eastward shift is most noticeable in UK-FOAM. Cooling in west is largely absent from GECCO which has reduced amplitude representations of some El Niños (possibly due to its choice of wind forcing). Indeed, the changes in stratification of the ensemble partly reflect (or express) the prevalence of El Niño events in the 1990s relative to the 1970s and the resulting eastward shift of warm water.

We next examine the representation of mode water formation in the subtropical North Pacific and Atlantic by comparison of the analyses to the long station time series records at Hawaii and Bermuda (we note that most of the analyses assimilate at least partial representations of these time series). In his examination of the Hawaii Ocean Time Series (at 23^{o}N, 158^{o}W) *Lukas (2001)* and *Lukas and Santiago-Mandujano (2008)* document a reduction and then increase in surface salinity as a result of several years of high rainfall 1995-7 followed by several years of low rainfall (**Fig. 7**, lower right). A

similar near surface salinity anomaly appears in most of the analyses even though different analyses use significantly different surface freshwater forcing estimates (**Table 1**). The weakest anomalies are apparent in those analyses, GODAS and SODA, which place the most restrictive constraints on salinity based on available temperature observations. In contrast, CERFACS and GFDL both have somewhat larger salinity anomalies at 300m and below than observed.

In the subtropical North Atlantic Station at S near Bermuda (32^{o}N, 64^{o}W) *Joyce and Robbins (1996)* document a similar multi-year fluctuation in water properties. Here in 1974-6 there was a reduction in mode water thickness indicated by an increase in potential vorticity (proportional to the vertical gradient of density) at 200m (**Fig. 8**, lower right). This high potential vorticity anomaly occurs in conjunction with an increase in the North Atlantic Oscillation Index and a succession of mild winters which limited mode water formation. This pattern of low, then high, then low potential vorticity is represented in all analyses. Interestingly, in INGV the high potential vorticity anomaly appears to propagate upward while in the others the anomaly propagates downward with time at this location (**Fig. 8**). Despite the encouraging similarity of the analyses at the location of Station S, the basin-scale representation of the anomalies (not shown) varies considerably with some analyses showing the anomaly at Bermuda to be basin-scale, while others showing the anomaly to be more local.

Finally we examine variability of upper ocean water properties in the North Atlantic subpolar gyre focusing on the quasi-decadal Great Salinity Anomaly freshening events of

the 1970s and 1980s. In the southern Labrador Sea (53°W-59°W, 50°N-56°N) near the location of ocean weather station Bravo these two Great Salinity Anomalies are evident in five of the nine analyses; CERFACS, INGV, SODA, UK-FOAM, and UK-OI; superimposed on a multi-decadal freshening trend (**Fig. 9a**, marked with arrows). In this region a third Great Salinity Anomaly of the early 1990s, noted by *Belkin (2004)*, is not clearly evident. These low salinity waters associated with the 1970s event are advected counterclockwise around the subpolar gyre, arriving in the Norwegian Basin near ocean weather station Mike (0-5°E, 63°N-69°N) seven years later (**Fig. 9b** marked with an arrow). All of the analyses that capture the Great Salinity Anomaly in the Labrador Sea in 1970; as well as one additional analysis, ECMWF; also show the later freshening event in the Norwegian Basin.

The spatial structure of the Great Salinity Anomaly during the early (1968-70) and middle years (1971-3) of this event is presented in **Fig. 10**. SODA and to a lesser extent CERFACS and INGV, show reductions in salinity along the coast of Greenland preceding the reduction in salinity within the Labrador Sea that are consistent with a freshwater source to the east of Greenland and advection through the East and West Greenland Currents. UK-OI and UK-FOAM, in contrast, show decreases in salinity in the Labrador Sea and western North Atlantic indicating a more local source of freshwater. Thus, the relative importance of advection and local sources of freshwater will likely vary depending on the resolution of the analysis.

4. Summary and Conclusions

This paper examines a selection of upper ocean water properties in the northern and tropical oceans during the years 1962-2001 as represented in an ensemble of nine ocean analyses. The analyses differ in the numerical models they use as well as surface forcing. The majority employ a form of sequential data assimilation applied to the ocean, but one uses 4DVar, one is a 'no model analysis', and one is a coupled atmosphere-ocean analysis. The data sets used to constrain the models also differ, for example with two including satellite altimetry and others not. Because of these many differences it is not possible to associate differences in the analyses definitively to differences in particular aspects of the assimilation system. Our approach is to explore representation of previously observed historical changes in water mass characteristics. Our focus is on sub-seasonal timescales and our goals are to identify similarity and differences of the analyses, and as a by-product to determine the extent to which our estimates of historical climate variability depend on analysis methodology, and finally to suggest causes for those differences. In brief, our conclusions are as follows:

1) The seasonal behavior of SST and mixed layer properties in the sequential and 4DVar analyses is qualitatively consistent with observations. The single no-model analysis, UK-OI, has very shallow mixed layers even in winter due to the presence of a shallow temperature inversion. In a couple of analyses anomalously cool winter-spring North Atlantic SSTs appear to allow the mixed layer in excessively large geographic regions to deepen into the layer containing North Atlantic Subtropical Mode Water. The mean properties of upper ocean constant density surfaces such as the 25.5 and 26.5σ surfaces are qualitatively correct for the sequential analyses and the no-model

analysis although most show a <10m anomalous deepening in the eastern North Pacific and a similar shallowing in the west. The GECCO 4DVar analysis shows a 10-30m basin-wide deepening of these isopycnal surfaces in the North Pacific in the 1990s.

2) We next examine subseasonal variability in the depth and salinity of the 25.5σ and 26.5σ isopycnal surfaces. For most analyses depth variability is mainly confined to regions of mode water mass formation and adjacent subtropical gyres. In the subtropical North Pacific a major component of this variability is the result of a succession of density anomalies formed in the northern North Pacific which travel clockwise around the subtropical gyre as previously described by *Miller and Schneider (2000)*. These anomalies are represented in a qualitatively similar way in all analyses. The 25.5σ surface in the North Pacific also shows a reduction in its zonal tilt between the 1970s and 1990s as the result of a deepening of the pycnocline in the east and a shallowing of the pycnocline in the west. This reduction in zonal tilt and associated reduction in vertical shear of meridional velocity *McPhaden and Zhang (2002)* associate with a slowing down of the shallow meridional overturning circulation. The sequential analyses generally show this change of slope extending to the equator, but the GECCO 4DVar analysis does not. The one analysis using a form of coupled assimilation, GFDL, shows significant multi-decadal near-surface freshening trends in some locations that do not appear in the other analyses.

3) The records of two time series, the Hawaii Ocean Time series in the North Pacific subtropical gyre and the Station S time series in the North Atlantic subtropical gyre are used to examine the response of the analyses to year-to-year changes in surface fluxes in the subtropics. In the North Pacific *Lukas (2001)* identifies a low salinity event spanning the years 1995-7. Comparison of the analyses at this location shows that most are able to reproduce this feature. Two analyses, SODA and GODAS, had weak anomalies as a result, we believe, of analysis procedures which limit variability of salinity in the presence of many temperature observations. In the North Atlantic all analyses are able to reproduce a reduction in North Atlantic Subtropical Mode Water thickness which occurred in the mid-1970s. However, the far field geographic representation of both the Pacific and Atlantic anomalies vary among the analyses.

4) Finally, we examine representation of the Great Salinity Anomalies of the North Atlantic supolar gyre. Five analyses; CERFACS, INGV, SODA, UK-FOAM, and UK-OI; show pronounced freshening events consistent with the observed record in both the Labrador Sea and the Norwegian Basin. The analysis with the highest spatial resolution, SODA, shows the most distinct advection of freshwater along the East and West Greenland Currents into the Labrador Sea.

This study follows an earlier examination by *Carton and Santorelli (2008)* of vertically averaged temperature which found substantial similarity among the analyses in the Northern Hemisphere. Here we consider vertically varying properties of both salinity and density and find more substantial variations among the analyses than were apparent

in the previous study. Many of the climate anomalies we examine are represented in multiple analyses and thus these analyses offer interesting opportunities for diagnostic examination. Significant differences between the analyses as well indicate that we can expect substantial refinements in the quality of ocean analyses in the near future.

Acknowledgement

The authors want to express their appreciation to the lead authors of the analyses used in this study: Magdalena Balmaseda, David Behringer, Mike Bell, Alessio Bellucci, Michael Davey, Benjamin Giese, Armin Köhl, Tony Lee, Tony Rosati, Chaojiao Sun, Zhaoqing Zhang, and their colleagues. This work was motivated by a series of workshops organized by Professor Detlef Stammer as part of the CLIVAR Global Synthesis and Observations Panel. Financial support for this research has been provided by the National Science Foundation (OCE0351319).

Reference

Adler, R.F., 2003: The version-2 global precipitation climatology project (GPCP) monthly precipitation analysis (1979-present), *J. Hydrolo.*, **4**, 1147-.

Balmaseda, M.A., G.C. Smith, K. Haines, D. Anderson, T.N. Palmer, and A. Vidard, 2007: Historical reconstruction of the Atlantic Meridional Overturning Circulation from the ECMWF operational ocean reanalysis, *Geophys. Res. Letts.*, **34**, #L23615.

Behringer, D.W., 2005: The global ocean data assimilation system (GODAS) at NCEP, 11th Symposium on Integrated Observing and Assimilation Systems for the Atmosphere, Oceans, and Land Surface (IOAS-AOLS), San Antonio, TX, *Amer. Meteor. Soc.*, **3.3**.

Belkin, I.M., 2004: Propagation of the ‘‘Great Salinity Anomaly’’ of the 1990s around the northern North Atlantic, *Geophys. Res. Letts.*, **31**, L08306, doi:10.1029/2003GL019334.

Bell, M.J., 2000: Assessment of the FOAM global data assimilation system for real-time operational ocean forecasting, *J. Marine Sys.*, **25**, 1-22.

Bell, M.J., M.J. Martin, and N.K. Nichols, 2004: Assimilation of data into an ocean model with systematic errors near the equator, *Quart. J. Roy. Meteor. Soc.*, **130**, 853-871.

Bellucci A., S. Masina, P. Di Pietro, and A. Navarra, 2007: Using temperature-salinity relations in a global ocean implementation of a multivariate data assimilation scheme. *Mon. Wea. Rev.*, **135**, 3785-3807.

Bingham, F., and T. Suga, 2006: Distributions of mixed layer properties in North Pacific water mass formation areas: comparison of Argo floats and World Ocean Atlas 2001. *Ocean Sci.*, **2**, 61-70.

Boyer, T.P., J.I. Antonov, H.E. Garcia, D.R. Johnson, R.A. Locarnini, A.V. Mishonov, M.T. Pitcher, O.K. Baranova, and I.V. Smolyar, 2006: World Ocean Database 2005. S. Levitus, Ed., NOAA Atlas NESDIS 60, U.S. Government Printing Office, Wash., D.C., 190pp.

Brambilla, E., and L. D. *Talley*, 2008: Subpolar Mode Water in the northeastern Atlantic: 1. Averaged properties and mean circulation, *J. Geophys. Res.*, **113**, C04025, doi:10.1029/2006JC004062.

Brambilla, Elena, Lynne D. Talley, and Paul E. Robbins, 2008: Subpolar Mode Water in the northeastern Atlantic: 2. Origin and transformation, *J. Geophys Res*, **113**, C04026, doi:10.1029/2006JC004063.

Carton, J.A., and A. Santorelli, 2008: Global Upper Ocean Heat Content as Viewed in Nine Analyses, *J. Clim.*, DOI: 10.1175/2008JCLI2489.1.

Carton, J.A., and B.S. Giese, 2008: A Reanalysis of Ocean Climate using SODA, *Mon. Wea. Rev.*, **136**, 2999–3017.

Carton, J.A., S.A. Grodsky, and H. Liu, 2008: Variability of the Oceanic Mixed Layer 1960-2004, *J. Clim.*, **5,** 1029-1047.

Climode Group, 2008: Observing the cycle of convection and restratification over the Gulf Stream system and the subtropical gyre of the North Atlantic ocean: preliminary results from the CLIMODE field campaign. *Bull. Amer. Meteor. Soc.*, submitted.

Davey, M., 2005: Enhanced Ocean Data Assimilation and Climate Prediction, European Commission Framework 5 Project Final Report, 79pp.

de Boyer Montégut, C., G. Madec, A. S. Fischer, A. Lazar, and D. Iudicone, 2004: Mixed layer depth over the global ocean: An examination of profile data and a profile-based climatology, *J. Geophys. Res.*, **109**, C12003, doi:10.1029/2004JC002378.

de Boyer Montégut, C., J. Mignot, A. Lazar, and S. Cravatte, 2007: Control of salinity on the mixed layer depth in the world ocean: 1. General description, *J. Geophys. Res.*, **112**, C06011,

Hanawa, K. and L.D. Talley, 2001: Mode Waters, in Ocean Circulation and Climate, Academic Press, 373-386.

Houghton, R.W., and M.H. Visbeck, 2002: Quasi-decadal salinity fluctuations in the Labrador Sea. *J. Phys. Oceanogr.*, **32**, 687–701.

Ingleby, B. and M. Huddleston, 2007: Quality control of ocean temperature and salinity profiles – historical and real time data, *J. Marine Sys.*, **65**, 158-175.

Joyce, T. M. and P. E. Robbins, 1996: The long-term hydrographic record at Bermuda, *J. Clim.*, **9**, 3121-3131.

Joyce, T. M., C. Deser, and M. A. Spall, 2000: The relation between decadal variability of subtropical mode water and the North Atlantic Oscillation. *J. Clim.*, **13**, 2550-2569.

Kalnay, E., and Coauthors, 1996: The NCEP/NCAR 40-year reanalysis project, *Bull. Amer. Meteorol. Soc.*, **77**, 437-471.

Kanamitsu, M., W. Ebisuzaki, J. Woollen, S-K Yang, J.J. Hnilo, M. Fiorino, and G. L. Potter, 2002: NCEP-DEO AMIP-II Reanalysis (R-2), *Bull. Amer. Meteor. Soc.*, **83**, 1631-1643.

Kleeman, R., J.P. McCreary, Jr., and B.A. Klinger, 1999: A mechanism for generating ENSO decadal variability, *Geophys. Res. Letts.*, **26**, 1743-1746.

Köhl, A., and D. Stammer, 2008: Decadal Sea Level Changes in the 50-Year GECCO Ocean Synthesis, *J. Clim.*, **21**, 1876-1890.

Lazier, J.R.N., 1995: The salinity decrease in the Labrador Sea over the past thirty years. In: Martinson, D.G., Bryan, K., Ghil, M., Hall, M.M., Karl, T.M., Sarachik, E.S., Sorooshian, S., Talley, L.D. (Eds.), Natural Climate Variability on Decade-to-Century Time Scales. National Academy Press, Washington, DC, pp. 295–302.

Lukas, R., 2001: Freshening of the upper thermocline in the North Pacific subtropical gyre associated with decadal changes of rainfall. *Geophys. Res. Letts.*, **28**, 485–488.

Lukas, R., and F. Santiago-Mandujano, 2008: Interannual to interdecadal salinity variations observed near Hawaii: local and remote forcing by surface freshwater fluxes, *Oceanogr.*, **21**, 46-55.

McPhaden, M. J., and D. Zhang, 2002: Slowdown of the meridional overturning circulation in the upper Pacific Ocean, *Nature*, **415**, 603–608.

Miller, A.J., and N. Schneider, 2000: Interdecadal climate regime dynamics in the North Pacific Ocean: theories, observations and ecosystem impacts. *Prog. Oceanogr.*, **47**, 355-379.

Nilsen, J.E.O., and E. Falck, 2003: Variations of mixed layer properties in the Norwegian Sea for the period 1948–1999, *Progr. Oceanogr.,* **70**, 58–90.

Nonaka, M., S.-P. Xie, and J.P. McCreary, 2002: Decadal variations in the subtropical cells and equatorial pacific SST, *Geophys. Res. Letts.*, **29**, 1116, 10.1029/2001GL013717.

Proshutinsky A. Y., and M. A. Johnson, 1997: Two circulation regimes of the wind-driven Arctic Ocean. *J. Geophys. Res.*, **102**, 12493–12514.

Ratsimandresy, A.W., J.L. Pelegri, A. Marrero-Diaz, A. Hernandez-Guerra, and A. Martinez, 2001: Seasonal variability of the upper warmwatersphere in the Canary Basin, *Scientia Marina*, **65**, 251-258.

Rayner, N.A., P. Brohan, D.E. Parker, C.K. Folland, J.J. Kennedy, M. Vanicek, T. Ansell, and S.F.B. Tett, 2006: Improved analyses of changes and uncertainties in sea surface temperature measured in situ since the mid-nineteenth century: the HadSST2 data set, *J. Clim.*, **19**, 446-469.

Schneider, N. 2004: The response of tropical climate to the equatorial emergence of spiciness anomalies, *J. Clim.*, **17**,1083-1095.

Siedler, G., A. Kuhl, and W. Zenk, 1987: The Madeira Mode Water, *J. Phys. Oceanogr.*, **13**, 828– 857.

Thadathil, P., A.K. Saran, V.V. Gopalakrishna, et al., 2002: XBT fall rate in waters of extreme temperature: a case study in the Antarctic Ocean, *J. Atmos. and Oceanic Tech.*, **19**, 391-396.

Uppala, S.M. and coauthors, 2005: The ERA-40 re-analysis, *Quart. J. R. Meteorol. Soc.*, **131**, 2961-3012. doi:10.1256/qj.04.176.

White, W.B., 1995: Design of a global observing system for gyre-scale upper ocean temperature variability, *Prog. Oceanogr.*, **36**, 169-217.

Yasuda, T., and K. Hanawa, 1997: Decadal Changes in the Mode Waters in the Midlatitude North Pacific, *J. Phys. Oceanogr.*, **27**, 858-870.

Zhang, S., M. J. Harrison, A. Rosati, and A. T. Wittenberg, 2007: System design and evaluation of coupled ensemble data assimilation for global oceanic climate studies, *Mon. Wea. Rev.*,**135**, 3541-3564.

Zhang, S., A. Rosati, and M. J. Harrison, 2008a: Detection of multi-decadal oceanic variability within a coupled ensemble data assimilation system. *J. Geophys. Res., accepted.*

Zhang, S., A. Rosati, M. J. Harrison, R. Gudge, and W. Stern, 2008b: GFDL's Coupled Ensemble Data Assimialtion System, 1980-2006 Oceanic Reanalysis and Its Impact on ENSO Forecasts. Preprint for wcrp3, Jan. 27 - Feb. 2, 2008, Tokyo (wcrp.ipsl.jussieu.fr/Workshops/Reanalysis2008/Documents/G4-434_ea.pdf).

Table 1 Analyses considered in this study. The vertical resolution given below only includes the number of levels between the surface and 700m. UK-FOAM has been shortened from 2004 to 1998 because of some problems at the end of the analysis period.

Analysis	Time Span	Surface fluxes			Model, res.	Analysis procedure
		Moment.	Heat	Fresh water		
CERFACS *Davey* (2005)	1962-2001	ERA-40 Reanal	ERA 40 Reanal	ERA-40 corrected in tropics	ORCA2 vers. OPA 2^ox2^o-$1/2^o$ 31 lev	Sequential
ECMWF *Balmaseda et al. (2007)*	1962-2001	ERA-40 Reanal	ERA 40 Reanal	ERA-40 corrected in tropics	HOPE 2^ox2^o-$1/2^o$ 21 lev	Sequential
GECCO *Köhl and Stammer (2008)*	1950-1999	NCEP Reanal	NCEP Reanal	NCEP Reanal	MITGCM 1^ox1^o 23 lev	4DVar
GFDL *Zhang et al. (2007; 2008a,b)*	1979-2002	Coupled	Coupled	Coupled	MOM4 1^ox1^o-$1/3^o$ 50 lev	Sequential
GODAS *Behringer* (2005)	1979-2005	NCEP Reanal.-2	NCEP Reanal.-2	NCEP Reanal.-2	MOM3 1^ox1^o-$1/3^o$ 40 lev	Sequential
INGV Bellucci, *et al. (2007)*	1962-2001	ERA-40 Reanal	ERA 40 Reanal	ERA-40 corrected in tropics	OPA 2^ox2^o-$1/2^o$ 31 lev	Sequential
SODA *Carton and Giese* (2008)	1958-2005	ERA-40 Reanal	bulk heat flux	GPCP rain	POP2.1 $1/4^o$x$1/4^o$ 40 lev	Sequential
UK-FOAM *Bell. (2000), Bell et al. (2004)*	1962-1998	ERA-40 Reanal	ERA 40 Reanal	ERA-40 corrected in tropics	GloSea 1^ox1^o-$1/3^o$ 20 lev	Sequential
UK-OI *Ingleby and Huddleston (2007)*	1962-2001				1^ox1^o	Objective Analysis

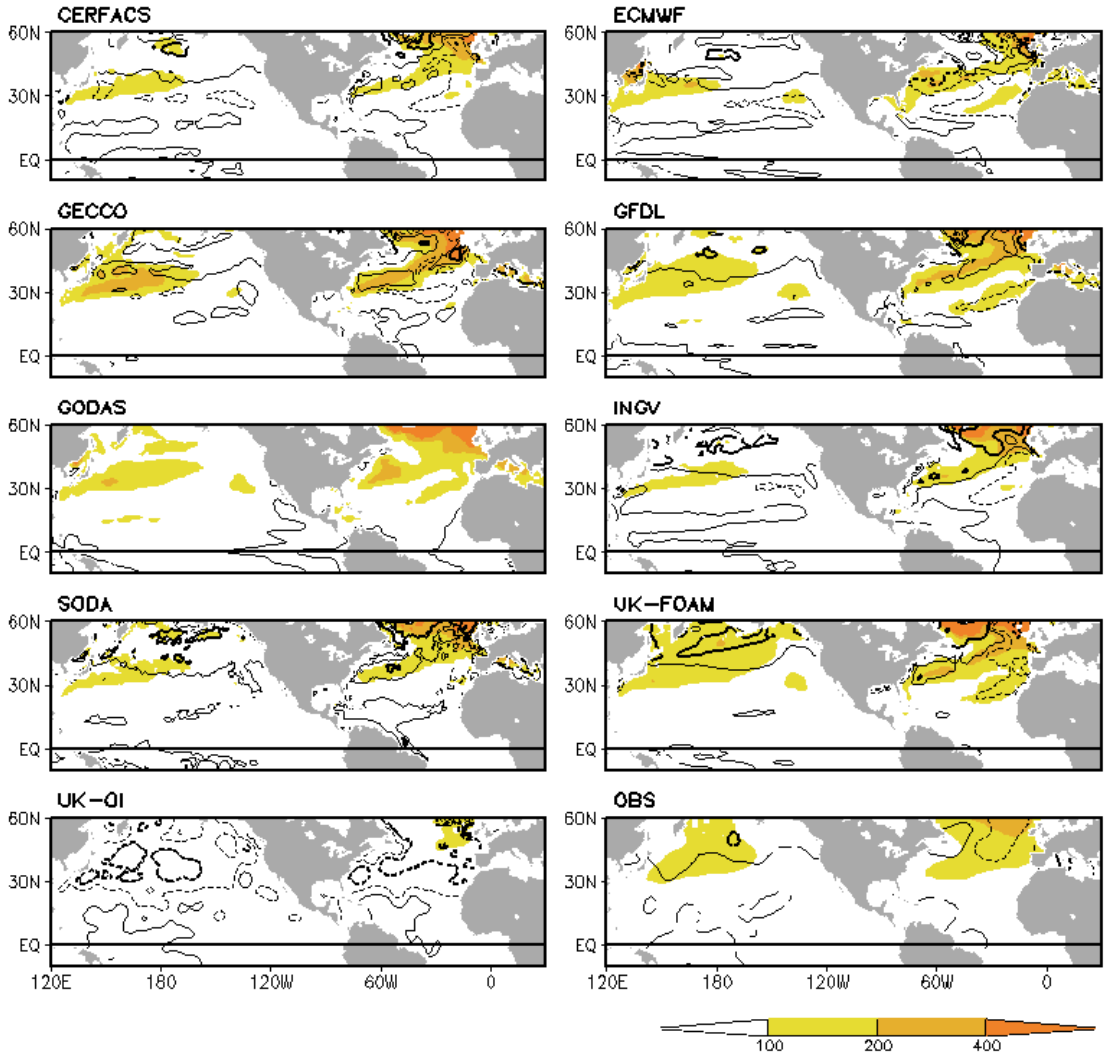

Figure 1a Winter-spring (JFM) mixed layer depth during the 16 year interval 1980-1995 computed using a 0.2°C absolute temperature criterion (colors in meters). Also shown is the difference between this depth and the depth of the mixed layer computed using an equivalent density criterion. Positive values of this difference indicate the thickness of a salinity barrier layer, while negative values indicate the thickness of a layer of temperature and salinity compensation (contours at ±10, ±30m, negative contours are dashed). Observations are from H. Liu *(personal communication, 2008)*.

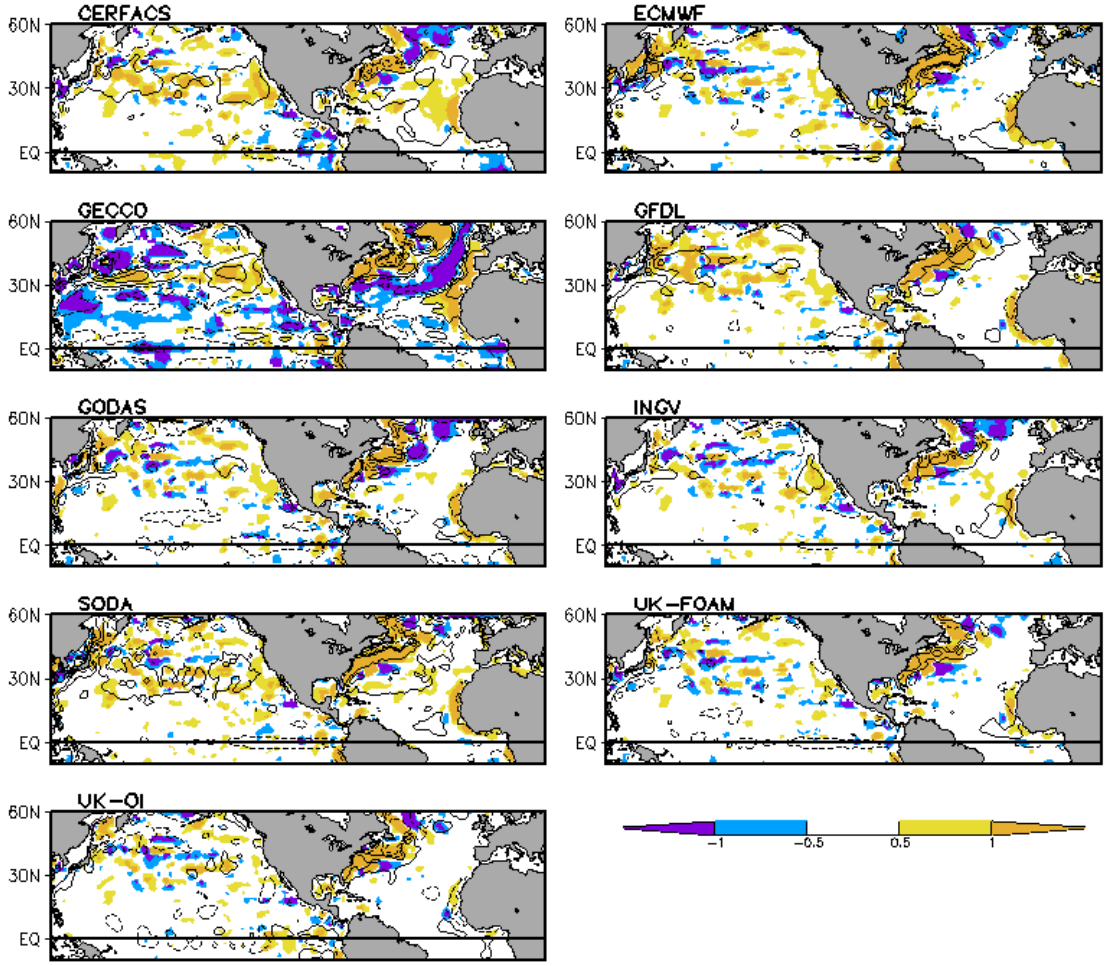

Figure 1b Winter-spring (JFM) SST difference (°C, analysis minus observation) computed during the 16 year interval 1980-1995. Colors show difference between the uppermost analysis level and a corresponding observation. Contours show the difference between the uppermost analysis level and the HADSST bulk SST analysis (contours at ±0.25 and ±1°C, negative contours dashed).

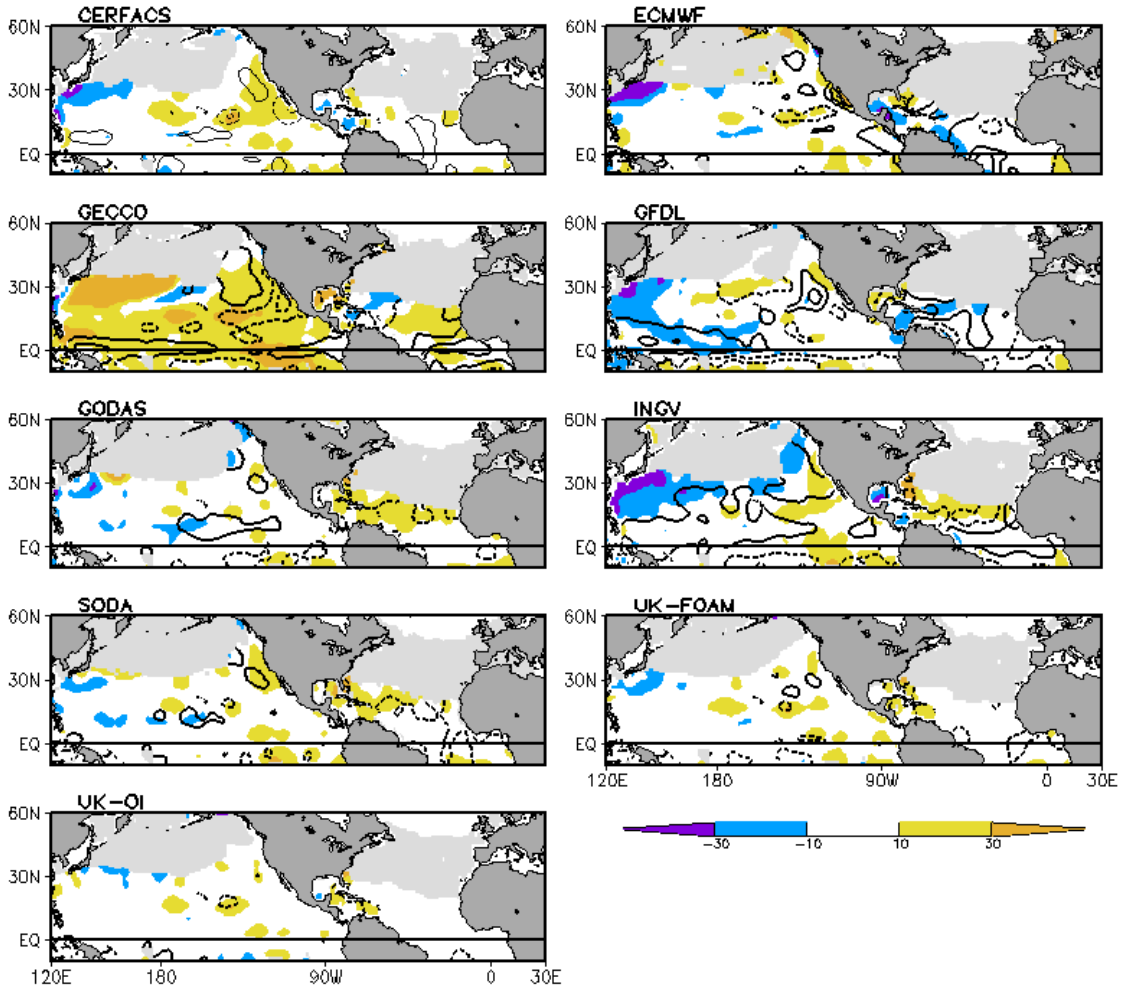

Figure 2 Time mean difference between analysis and observation properties of the 25.5σ surface of the depth computed during the 16-year period 1980-1995. Depth difference is shown in color (m) and salinity difference in contours (±0.1, ±0.3psu, negative contours are dashed). Grey areas define seasonal outcropping regions.

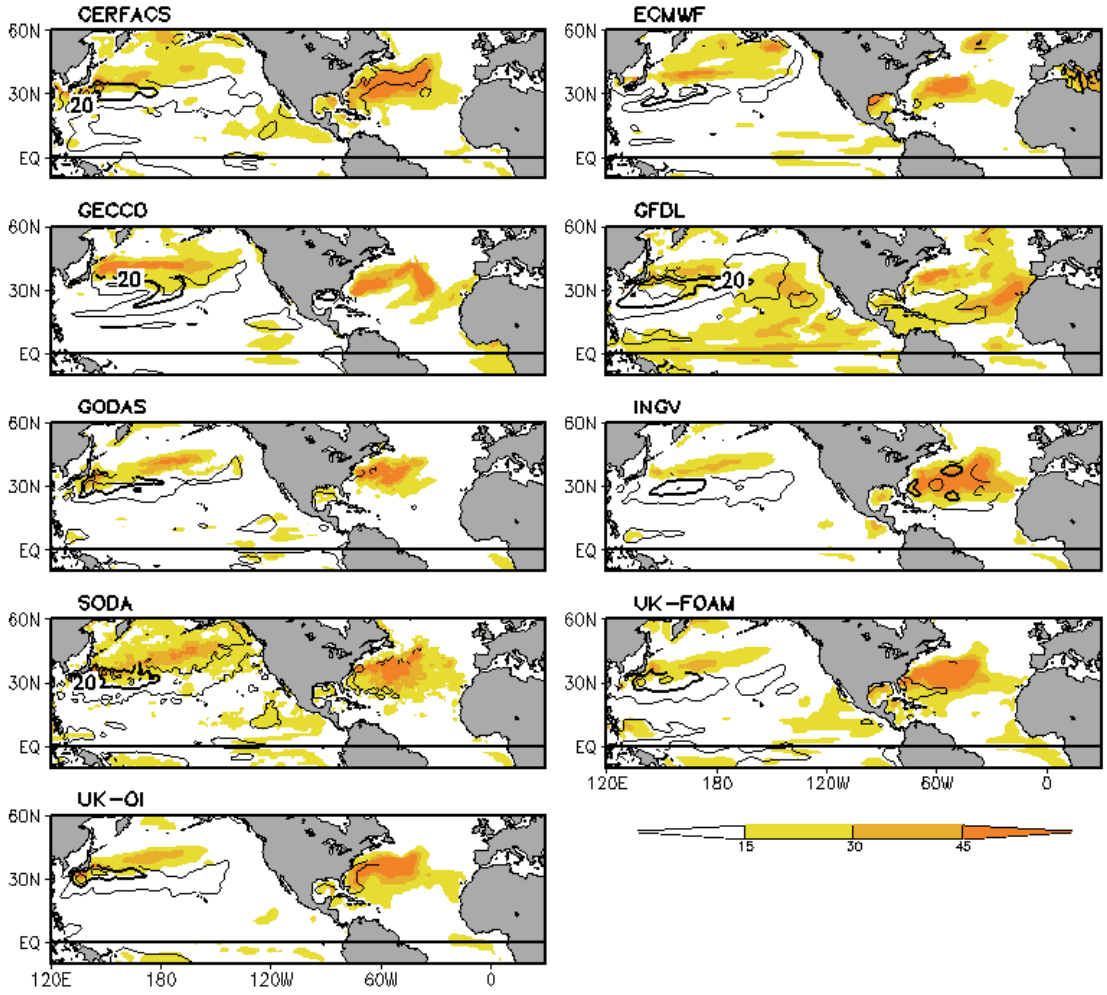

Figure 3 Root-mean-square variability of the depth of constant density surfaces (3-yr low pass filtered) computed over the full analysis period. Colors show the RMS depth of the 26.5σ surface. Contours show the RMS depth of the 25.5σ surface (contour interval is 10m, 20m contour is bold).

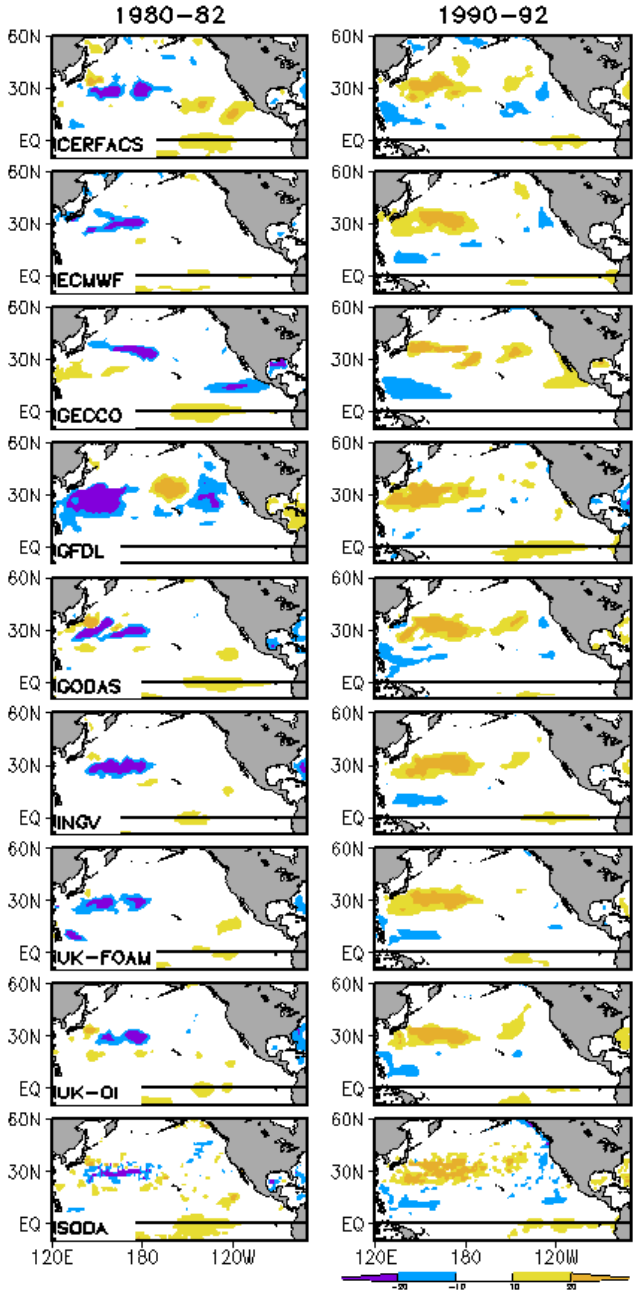

Figure 4 Depth anomaly (m) of the 25.5σ surface relative to the 1980-1995 average for two 3-year periods, 1980-82 and 1990-92 (following *Miller and Schneider, 2000*), when the decadal cycle of North Pacific variability was in opposite phases.

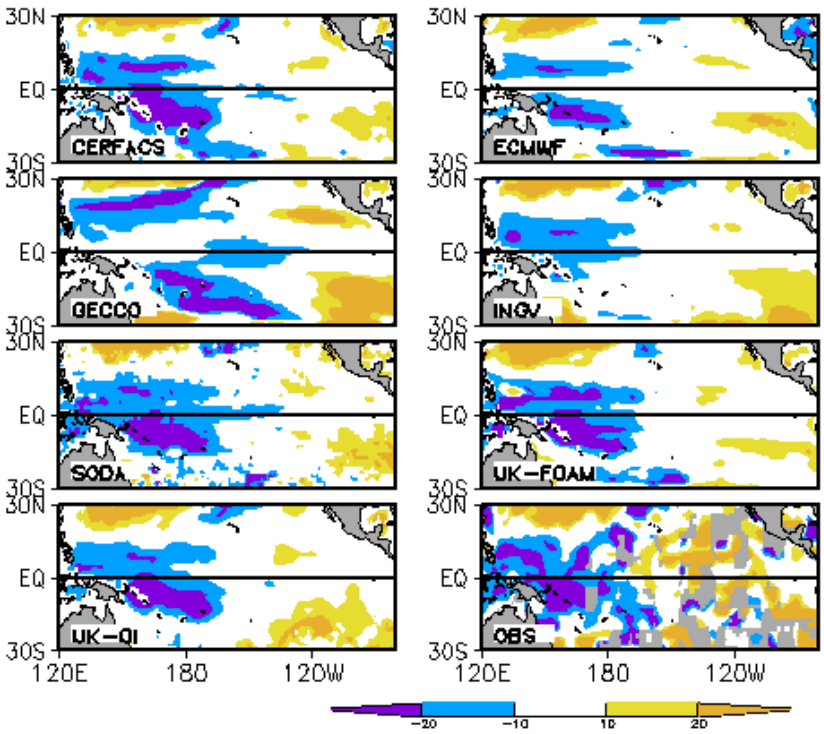

Figure 5 Change in depth (m) of the 25.5σ surface averaged 1990-1999 minus 1970-1977. Observations (lower right) show a deepening in the east and a shallowing in the west (see *McPhaden and Zhang, 2002* for discussion). Grey regions indicate limited CTD and station sampling.

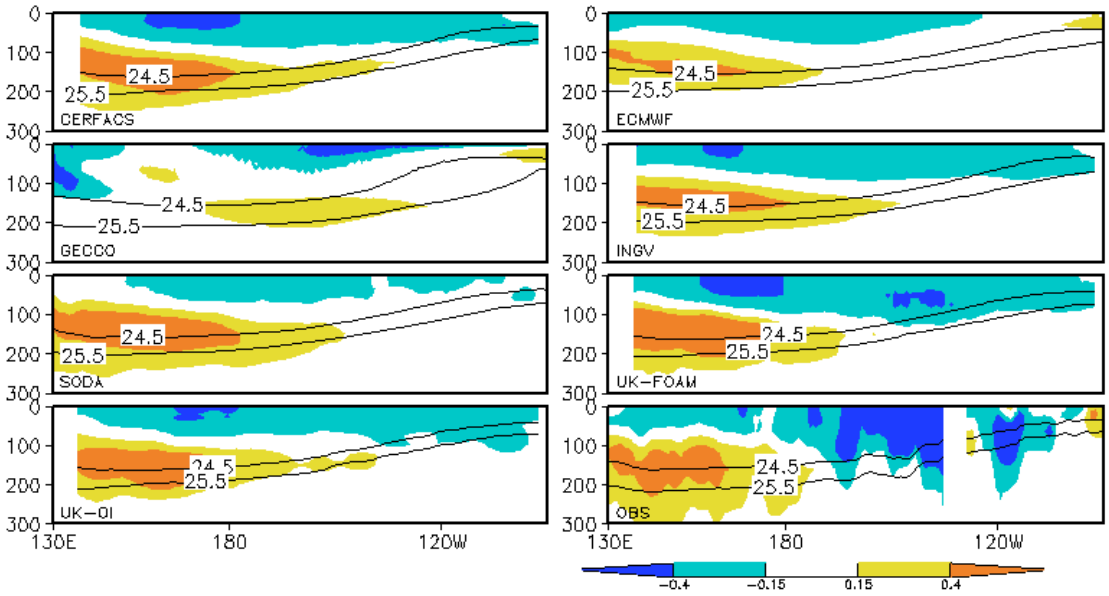

Figure 6 Change in density (kg m^{-3}) averaged 1990-1999 minus 1970-1977 along the equator in the Pacific as a function of depth. Depth of the mean 24.5σ and 25.5σ surfaces are superimposed.

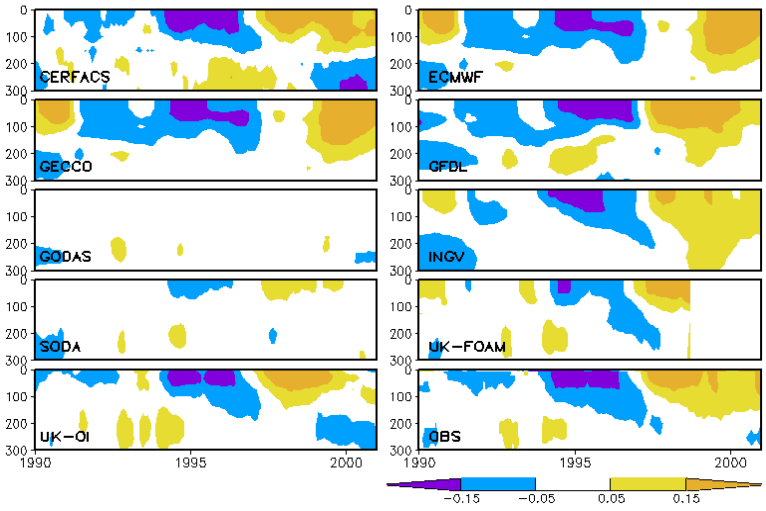

Figure 7 Salinity anomaly from the 1990-2001 average with depth averaged horizontally in a 2^{o}x2^{o} box centered on the location of the Hawaii Ocean Time Series (23^{o}N, 158^{o}W) and in time with a 6-month running filter. Observations (lower right) show a fresh and then salty anomaly appearing first at the surface and then extending into the water column to 200m depth (see *Lukas, 2002* for discussion).

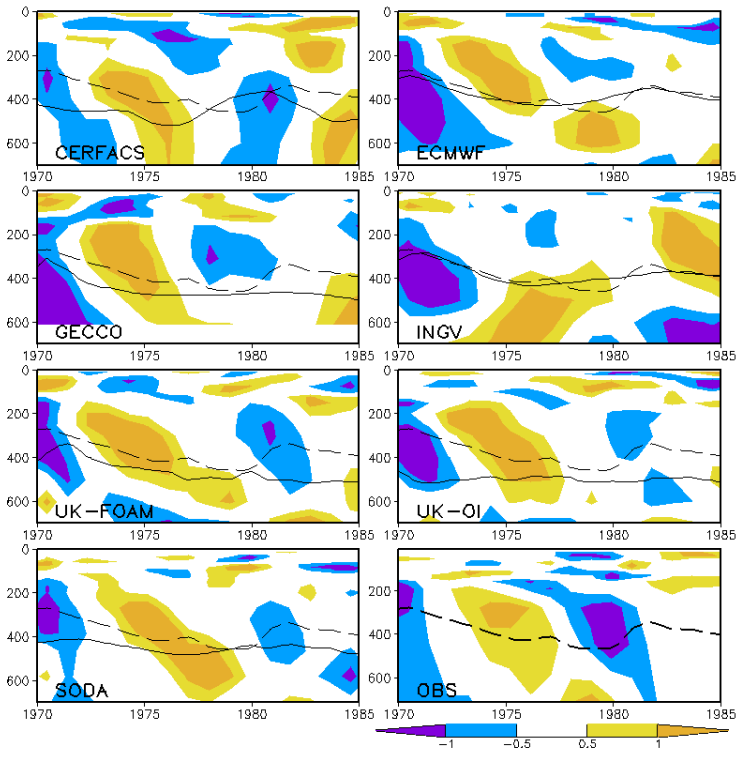

Figure 8 Potential vorticity anomaly (normalized by PV variability at each level) from the 1970-1985 average, averaged in a 2^{o}x2^{o} box centered on the location of Station S (32^{o}N, 64^{o}W) and in time with an annual filter. Solid line indicates depth of the 26.5σ surface in each analysis. Observations (lower right) show a succession of high and low potential vorticity events (see *Joyce and Robbins, 1996* for discussion).

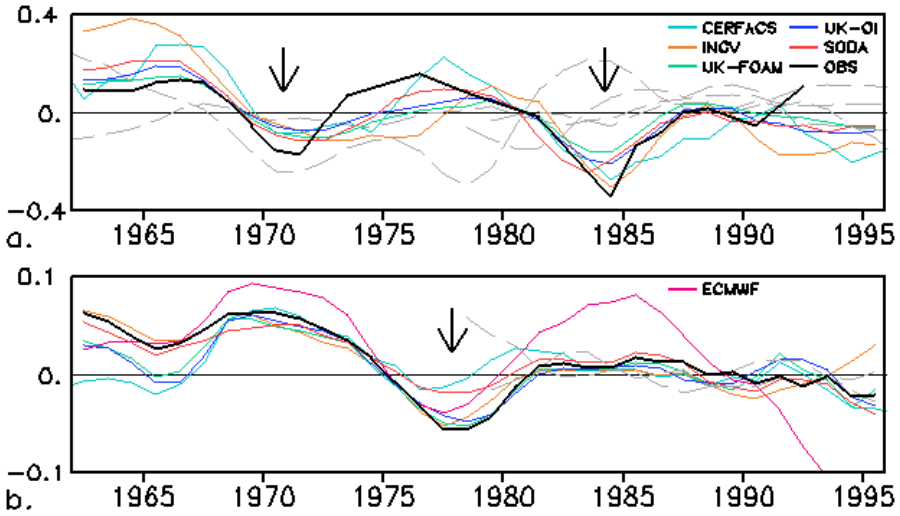

Figure 9 Annually averaged salinity anomaly from the 1962-1995 average, averaged horizontally and vertically in two regions. **a)** Labrador Sea (53°W-59°W, 50°N-56°N) averaged vertically (0-250m). Observations (black solid) are from *Lazier, 1995*). Two 'Great Salinity Anomaly' decreases are apparent 1967-1971 and again 1978-1985 (see *Lazier, 1995* for discussion). **b)** Norwegian Basin (0-5°E, 63°N-69°N) averaged vertically (0-500m). The Great Salinity Anomaly which appeared in the Labrador Sea in early 1970s appears at this location in the late 1970s (see *Nilsen and Falck, 2003* for discussion).

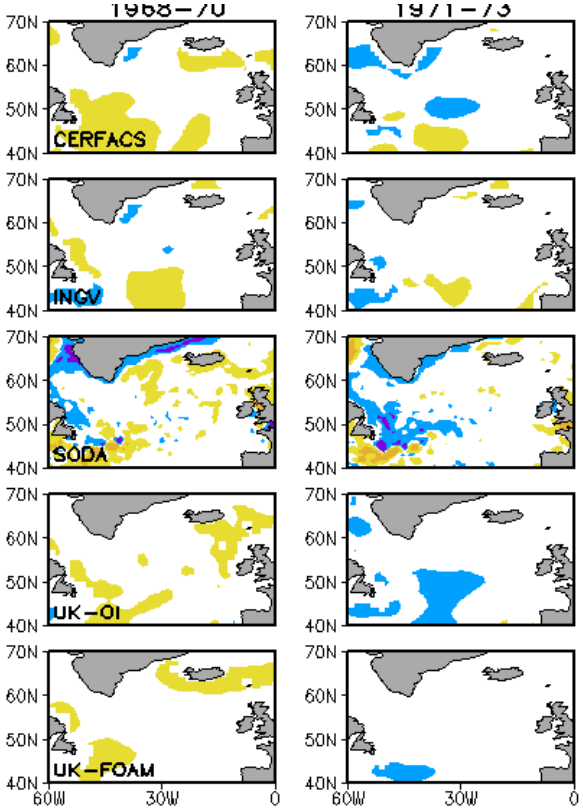

Figure 10 Salinity anomaly from the 1962-1995 average, averaged vertically (0-250m) and in time for three 3-year periods 1968-70 and 1971-3 for the analyses shown in color in **Fig. 9a**. The first two periods show early and mid stages of the 1970s Great Salinity Anomaly, while the third period shows the mid-stage of the 1980s Great Salinity Anomaly**.**